



## Measurement of the $\tau$ -lepton lifetime at Belle

K. Belous,<sup>17</sup> M. Shapkin,<sup>17</sup> A. Sokolov,<sup>17</sup> I. Adachi,<sup>10</sup> H. Aihara,<sup>58</sup> D. M. Asner,<sup>45</sup>  
 V. Aulchenko,<sup>3</sup> A. M. Bakich,<sup>52</sup> A. Bala,<sup>46</sup> B. Bhuyan,<sup>13</sup> A. Bobrov,<sup>3</sup> A. Bondar,<sup>3</sup>  
 G. Bonvicini,<sup>64</sup> A. Bozek,<sup>40</sup> M. Bračko,<sup>29,20</sup> T. E. Browder,<sup>9</sup> D. Červenkov,<sup>4</sup>  
 V. Chekelian,<sup>30</sup> A. Chen,<sup>37</sup> B. G. Cheon,<sup>8</sup> K. Chilikin,<sup>19</sup> R. Chistov,<sup>19</sup> K. Cho,<sup>23</sup>  
 V. Chobanova,<sup>30</sup> Y. Choi,<sup>51</sup> D. Cinabro,<sup>64</sup> J. Dalseno,<sup>30,54</sup> Z. Doležal,<sup>4</sup> D. Dutta,<sup>13</sup>  
 S. Eidelman,<sup>3</sup> D. Epifanov,<sup>58</sup> H. Farhat,<sup>64</sup> J. E. Fast,<sup>45</sup> T. Ferber,<sup>6</sup> V. Gaur,<sup>53</sup>  
 S. Ganguly,<sup>64</sup> A. Garmash,<sup>3</sup> R. Gillard,<sup>64</sup> Y. M. Goh,<sup>8</sup> B. Golob,<sup>27,20</sup> J. Haba,<sup>10</sup> T. Hara,<sup>10</sup>  
 K. Hayasaka,<sup>35</sup> H. Hayashii,<sup>36</sup> Y. Hoshi,<sup>56</sup> W.-S. Hou,<sup>39</sup> T. Iijima,<sup>35,34</sup> K. Inami,<sup>34</sup>  
 A. Ishikawa,<sup>57</sup> R. Itoh,<sup>10</sup> T. Iwashita,<sup>36</sup> I. Jaegle,<sup>9</sup> T. Julius,<sup>31</sup> E. Kato,<sup>57</sup> H. Kichimi,<sup>10</sup>  
 C. Kiesling,<sup>30</sup> D. Y. Kim,<sup>50</sup> H. J. Kim,<sup>25</sup> J. B. Kim,<sup>24</sup> M. J. Kim,<sup>25</sup> Y. J. Kim,<sup>23</sup>  
 K. Kinoshita,<sup>5</sup> B. R. Ko,<sup>24</sup> P. Kodyš,<sup>4</sup> S. Korpar,<sup>29,20</sup> P. Križan,<sup>27,20</sup> P. Krokovny,<sup>3</sup>  
 T. Kuhr,<sup>22</sup> A. Kuzmin,<sup>3</sup> Y.-J. Kwon,<sup>66</sup> J. S. Lange,<sup>7</sup> S.-H. Lee,<sup>24</sup> J. Libby,<sup>14</sup> D. Liventsev,<sup>10</sup>  
 P. Lukin,<sup>3</sup> D. Matvienko,<sup>3</sup> H. Miyata,<sup>42</sup> R. Mizuk,<sup>19,32</sup> G. B. Mohanty,<sup>53</sup> T. Mori,<sup>34</sup>  
 R. Mussa,<sup>18</sup> Y. Nagasaka,<sup>11</sup> E. Nakano,<sup>44</sup> M. Nakao,<sup>10</sup> M. Nayak,<sup>14</sup> E. Nedelkovska,<sup>30</sup>  
 C. Ng,<sup>58</sup> N. K. Nisar,<sup>53</sup> S. Nishida,<sup>10</sup> O. Nitoh,<sup>61</sup> S. Ogawa,<sup>55</sup> S. Okuno,<sup>21</sup> S. L. Olsen,<sup>49</sup>  
 W. Ostrowicz,<sup>40</sup> G. Pakhlova,<sup>19</sup> C. W. Park,<sup>51</sup> H. Park,<sup>25</sup> H. K. Park,<sup>25</sup> T. K. Pedlar,<sup>28</sup>  
 R. Pestotnik,<sup>20</sup> M. Petrič,<sup>20</sup> L. E. Piilonen,<sup>63</sup> M. Ritter,<sup>30</sup> M. Röhrken,<sup>22</sup> A. Rostomyan,<sup>6</sup>  
 S. Ryu,<sup>49</sup> H. Sahoo,<sup>9</sup> T. Saito,<sup>57</sup> Y. Sakai,<sup>10</sup> S. Sandilya,<sup>53</sup> D. Santel,<sup>5</sup> L. Santelj,<sup>20</sup>  
 T. Sanuki,<sup>57</sup> V. Savinov,<sup>47</sup> O. Schneider,<sup>26</sup> G. Schnell,<sup>1,12</sup> C. Schwanda,<sup>16</sup> D. Semmler,<sup>7</sup>  
 K. Senyo,<sup>65</sup> O. Seon,<sup>34</sup> V. Shebalin,<sup>3</sup> C. P. Shen,<sup>2</sup> T.-A. Shibata,<sup>59</sup> J.-G. Shiu,<sup>39</sup>  
 B. Shwartz,<sup>3</sup> A. Sibidanov,<sup>52</sup> F. Simon,<sup>30,54</sup> Y.-S. Sohn,<sup>66</sup> S. Stanič,<sup>43</sup> M. Starič,<sup>20</sup>  
 M. Steder,<sup>6</sup> T. Sumiyoshi,<sup>60</sup> U. Tamponi,<sup>18,62</sup> G. Tatishvili,<sup>45</sup> Y. Teramoto,<sup>44</sup> K. Trabelsi,<sup>10</sup>  
 T. Tsuboyama,<sup>10</sup> M. Uchida,<sup>59</sup> S. Uehara,<sup>10</sup> T. Uglov,<sup>19,33</sup> Y. Unno,<sup>8</sup> S. Uno,<sup>10</sup>  
 Y. Usov,<sup>3</sup> S. E. Vahsen,<sup>9</sup> C. Van Hulse,<sup>1</sup> P. Vanhoefer,<sup>30</sup> G. Varner,<sup>9</sup> K. E. Varvell,<sup>52</sup>  
 A. Vinokurova,<sup>3</sup> V. Vorobyev,<sup>3</sup> M. N. Wagner,<sup>7</sup> C. H. Wang,<sup>38</sup> P. Wang,<sup>15</sup> M. Watanabe,<sup>42</sup>

Y. Watanabe,<sup>21</sup> K. M. Williams,<sup>63</sup> E. Won,<sup>24</sup> J. Yamaoka,<sup>9</sup> Y. Yamashita,<sup>41</sup>  
S. Yashchenko,<sup>6</sup> Y. Yook,<sup>66</sup> C. Z. Yuan,<sup>15</sup> Z. P. Zhang,<sup>48</sup> V. Zhilich,<sup>3</sup> and A. Zupanc<sup>22</sup>

(The Belle Collaboration)

<sup>1</sup>*University of the Basque Country UPV/EHU, 48080 Bilbao*

<sup>2</sup>*Beihang University, Beijing 100191*

<sup>3</sup>*Budker Institute of Nuclear Physics SB RAS and  
Novosibirsk State University, Novosibirsk 630090*

<sup>4</sup>*Faculty of Mathematics and Physics, Charles University, 121 16 Prague*

<sup>5</sup>*University of Cincinnati, Cincinnati, Ohio 45221*

<sup>6</sup>*Deutsches Elektronen-Synchrotron, 22607 Hamburg*

<sup>7</sup>*Justus-Liebig-Universität Gießen, 35392 Gießen*

<sup>8</sup>*Hanyang University, Seoul 133-791*

<sup>9</sup>*University of Hawaii, Honolulu, Hawaii 96822*

<sup>10</sup>*High Energy Accelerator Research Organization (KEK), Tsukuba 305-0801*

<sup>11</sup>*Hiroshima Institute of Technology, Hiroshima 731-5193*

<sup>12</sup>*Ikerbasque, 48011 Bilbao*

<sup>13</sup>*Indian Institute of Technology Guwahati, Assam 781039*

<sup>14</sup>*Indian Institute of Technology Madras, Chennai 600036*

<sup>15</sup>*Institute of High Energy Physics,*

*Chinese Academy of Sciences, Beijing 100049*

<sup>16</sup>*Institute of High Energy Physics, Vienna 1050*

<sup>17</sup>*Institute for High Energy Physics, Protvino 142281*

<sup>18</sup>*INFN - Sezione di Torino, 10125 Torino*

<sup>19</sup>*Institute for Theoretical and Experimental Physics, Moscow 117218*

<sup>20</sup>*J. Stefan Institute, 1000 Ljubljana*

<sup>21</sup>*Kanagawa University, Yokohama 221-8686*

<sup>22</sup>*Institut für Experimentelle Kernphysik,*

*Karlsruher Institut für Technologie, 76131 Karlsruhe*

<sup>23</sup>*Korea Institute of Science and Technology Information, Daejeon 305-806*

<sup>24</sup>*Korea University, Seoul 136-713*

<sup>25</sup>*Kyungpook National University, Daegu 702-701*

- <sup>26</sup>*École Polytechnique Fédérale de Lausanne (EPFL), Lausanne 1015*
- <sup>27</sup>*Faculty of Mathematics and Physics,  
University of Ljubljana, 1000 Ljubljana*
- <sup>28</sup>*Luther College, Decorah, Iowa 52101*
- <sup>29</sup>*University of Maribor, 2000 Maribor*
- <sup>30</sup>*Max-Planck-Institut für Physik, 80805 München*
- <sup>31</sup>*School of Physics, University of Melbourne, Victoria 3010*
- <sup>32</sup>*Moscow Physical Engineering Institute, Moscow 115409*
- <sup>33</sup>*Moscow Institute of Physics and Technology, Moscow Region 141700*
- <sup>34</sup>*Graduate School of Science, Nagoya University, Nagoya 464-8602*
- <sup>35</sup>*Kobayashi-Maskawa Institute, Nagoya University, Nagoya 464-8602*
- <sup>36</sup>*Nara Women's University, Nara 630-8506*
- <sup>37</sup>*National Central University, Chung-li 32054*
- <sup>38</sup>*National United University, Miao Li 36003*
- <sup>39</sup>*Department of Physics, National Taiwan University, Taipei 10617*
- <sup>40</sup>*H. Niewodniczanski Institute of Nuclear Physics, Krakow 31-342*
- <sup>41</sup>*Nippon Dental University, Niigata 951-8580*
- <sup>42</sup>*Niigata University, Niigata 950-2181*
- <sup>43</sup>*University of Nova Gorica, 5000 Nova Gorica*
- <sup>44</sup>*Osaka City University, Osaka 558-8585*
- <sup>45</sup>*Pacific Northwest National Laboratory, Richland, Washington 99352*
- <sup>46</sup>*Panjab University, Chandigarh 160014*
- <sup>47</sup>*University of Pittsburgh, Pittsburgh, Pennsylvania 15260*
- <sup>48</sup>*University of Science and Technology of China, Hefei 230026*
- <sup>49</sup>*Seoul National University, Seoul 151-742*
- <sup>50</sup>*Soongsil University, Seoul 156-743*
- <sup>51</sup>*Sungkyunkwan University, Suwon 440-746*
- <sup>52</sup>*School of Physics, University of Sydney, NSW 2006*
- <sup>53</sup>*Tata Institute of Fundamental Research, Mumbai 400005*
- <sup>54</sup>*Excellence Cluster Universe, Technische Universität München, 85748 Garching*
- <sup>55</sup>*Toho University, Funabashi 274-8510*
- <sup>56</sup>*Tohoku Gakuin University, Tagajo 985-8537*

<sup>57</sup>*Tohoku University, Sendai 980-8578*

<sup>58</sup>*Department of Physics, University of Tokyo, Tokyo 113-0033*

<sup>59</sup>*Tokyo Institute of Technology, Tokyo 152-8550*

<sup>60</sup>*Tokyo Metropolitan University, Tokyo 192-0397*

<sup>61</sup>*Tokyo University of Agriculture and Technology, Tokyo 184-8588*

<sup>62</sup>*University of Torino, 10124 Torino*

<sup>63</sup>*CNP, Virginia Polytechnic Institute and State University, Blacksburg, Virginia 24061*

<sup>64</sup>*Wayne State University, Detroit, Michigan 48202*

<sup>65</sup>*Yamagata University, Yamagata 990-8560*

<sup>66</sup>*Yonsei University, Seoul 120-749*

## Abstract

The lifetime of the  $\tau$ -lepton is measured using the process  $e^+e^- \rightarrow \tau^+\tau^-$ , where both  $\tau$ -leptons decay to  $3\pi\nu_\tau$ . The result for the mean lifetime, based on  $711\text{ fb}^{-1}$  of data collected with the Belle detector at the  $\Upsilon(4S)$  resonance and 60 MeV below, is  $\tau = (290.17 \pm 0.53(\text{stat.}) \pm 0.33(\text{syst.})) \cdot 10^{-15}\text{ s}$ . The first measurement of the lifetime difference between  $\tau^+$  and  $\tau^-$  is performed. The upper limit on the relative lifetime difference between positive and negative  $\tau$ -leptons is  $|\Delta\tau|/\tau < 7.0 \times 10^{-3}$  at 90% CL.

PACS numbers: 13.66.Jn, 14.60.Fq

## I. INTRODUCTION

High precision measurements of the mass, lifetime and leptonic branching fractions of the  $\tau$ -lepton can be used to test lepton universality [1], which is assumed in the Standard Model. Among the recent experimental results that may manifest the violation of the lepton universality in the case of the  $\tau$ -lepton, the combined measurement of the ratio of the branching fraction of  $W$ -boson decay to  $\tau\nu_\tau$  to the mean branching fraction of  $W$ -boson decay to  $\mu\nu_\mu$  and  $e\nu_e$  by the four LEP experiments stands out:  $2\mathcal{B}(W \rightarrow \tau\nu_\tau)/(\mathcal{B}(W \rightarrow \mu\nu_\mu) + \mathcal{B}(W \rightarrow e\nu_e)) = 1.066 \pm 0.025$  [2], which differs from unity by 2.6 standard deviations. The present PDG value of the  $\tau$ -lepton lifetime  $(290.6 \pm 1.0) \cdot 10^{-15}$  s [3] is dominated by the results obtained in the LEP experiments [4].

A high-statistics data sample collected at Belle allows us to select  $\tau^+\tau^-$  events where both  $\tau$ -leptons decay to three charged pions and a neutrino. As explained later, for these events the directions of the  $\tau$ -leptons can be determined with an accuracy better than that given by the thrust axis of the event. At an asymmetric-energy collider, the laboratory frame angle between the produced  $\tau$ -leptons is not equal to 180 degrees, so their production point can be determined from the intersection of two trajectories defined by the  $\tau$ -lepton decay vertices and their momentum directions. The direction of each  $\tau$ -lepton in the laboratory system can be determined with twofold ambiguity. These special features of the asymmetric-energy B-factory experiments allow a high precision measurement of the  $\tau$ -lepton lifetime with systematic uncertainties that differ from those of the LEP experiments.

Furthermore, Belle's asymmetric-energy collisions provide a unique possibility to measure separately the  $\tau^+$  and  $\tau^-$  lifetimes, which allows us to test  $CPT$  symmetry in  $\tau$ -lepton decays.

## II. DESCRIPTION OF THE MEASUREMENT METHOD AND SELECTION CRITERIA

In the following, we use symbols with and without an asterisk for quantities in the  $e^+e^-$  center-of-mass (CM) and laboratory frame, respectively. In the CM frame,  $\tau^+$  and  $\tau^-$  leptons emerge back to back with the energy  $E_\tau^*$  equal to the beam energy  $E_{\text{beam}}^*$  if we neglect the initial- (ISR) and final-state radiation (FSR). We determine the direction of the  $\tau$ -lepton momentum in the CM frame as follows. If the neutrino mass is assumed to be zero

for the hadronic decay  $\tau \rightarrow X\nu_\tau$  ( $X$  representing the hadronic system with mass  $m_X$  and energy  $E_X^*$ ), the angle  $\theta^*$  between the momentum  $\vec{P}_X^*$  of the hadronic system and that of the  $\tau$ -lepton is given by:

$$\cos \theta^* = \frac{2E_\tau^* E_X^* - m_\tau^2 - m_X^2}{2P_X^* \sqrt{(E_\tau^*)^2 - m_\tau^2}}. \quad (1)$$

The requirement that the  $\tau$ -leptons be back to back in the CM can be written as a system of three equations: two linear and one quadratic. For the components  $x^*, y^*, z^*$  of the unit vector  $\hat{n}_+^*$  representing the direction of the positive  $\tau$ -lepton, we write:

$$\begin{cases} x^* \cdot P_{1x}^* + y^* \cdot P_{1y}^* + z^* \cdot P_{1z}^* = |P_1^*| \cos \theta_1^* \\ x^* \cdot P_{2x}^* + y^* \cdot P_{2y}^* + z^* \cdot P_{2z}^* = -|P_2^*| \cos \theta_2^* \\ (x^*)^2 + (y^*)^2 + (z^*)^2 = 1 \end{cases} \quad (2)$$

where  $\vec{P}_1^*$  and  $\vec{P}_2^*$  are the momenta of the hadronic systems in the CM and  $\cos \theta_i^*$  ( $i = 1, 2$ ) are given by Eq. (1). Index 1 (2) is used for the positive (negative)  $\tau$ -lepton.

There are two solutions for Eq. (2), so the direction  $\hat{n}_+^*$  is determined with twofold ambiguity. In the present analysis, we take the mean vector of the two solutions of Eq. (2) as the direction of the  $\tau$ -lepton in CM. The analysis of MC simulated events shows that there is no bias due to this choice.

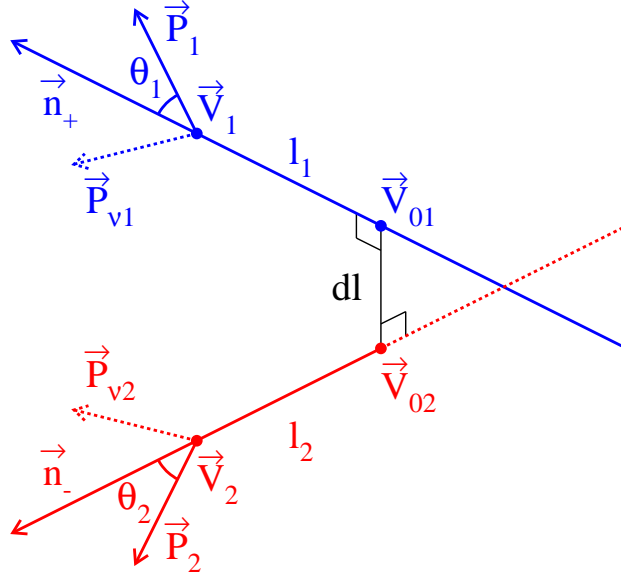


FIG. 1. The schematic view of the  $\tau^+\tau^-$  event in the laboratory frame.

Each direction  $\hat{n}_\pm^*$  is converted to a four-momentum using the  $e^\pm$  beam energy and the  $\tau$  mass. Both four-momenta are then boosted into the laboratory frame, each passing through

the corresponding  $\tau$  decay vertex  $\vec{V}_i$  that is determined by the three pion-daughter tracks (see Fig. 1). We approximate the trajectory of  $\tau$ -leptons in the magnetic field of the Belle detector with a straight line. Due to the finite detector resolution, these straight lines do not intersect at the  $\tau^+\tau^-$  production point. The three-dimensional separation between these lines is characterized by the distance  $dl$  between the two points ( $\vec{V}_{01}$  and  $\vec{V}_{02}$ ) of closest approach. The typical size of  $dl$  is  $\sim 0.01$  cm. For the production point of each  $\tau$ -lepton, we take the points  $\vec{V}_{01}$  and  $\vec{V}_{02}$ . The flight distance  $l_1$  ( $l_2$ ) of the  $\tau^+$  ( $\tau^-$ ) in the laboratory frame is defined as the distance between the points  $\vec{V}_1$  and  $\vec{V}_{01}$  ( $\vec{V}_2$  and  $\vec{V}_{02}$ ). The proper time  $t$  (the product of the speed of light and the decay time of  $\tau$ -lepton) for the positive  $\tau$ -lepton is equal to the distance  $l_1$  divided by its relativistic kinematic factor  $\beta\gamma$  in the laboratory frame:  $t_1 = l_1/(\beta\gamma)_1$ . The corresponding parameter for the negative  $\tau$ -lepton is  $t_2 = l_2/(\beta\gamma)_2$ .

The analysis presented here is based on the data collected with the Belle detector [5] at the KEKB asymmetric-energy  $e^+e^-$  (3.5 on 8 GeV) collider [6] operating at the  $\Upsilon(4S)$  resonance and 60 MeV below. The total integrated luminosity of the data sample used in the analysis is  $711 \text{ fb}^{-1}$ . Two inner detector configurations were used. A 2.0 cm beampipe and a 3-layer silicon vertex detector (SVD1) were used for the first sample of  $157 \text{ fb}^{-1}$ , while a 1.5 cm beampipe, a 4-layer silicon detector (SVD2) and a small-cell inner drift chamber were used to record the remaining  $554 \text{ fb}^{-1}$  [7]. The integrated luminosity of the data sample at the energy below the  $\Upsilon(4S)$  resonance is about 10% of the total data sample. All analyzed distributions for the on- and off-resonance data coincide within the statistical uncertainties with each other; this justifies our combination of the on- and off-resonance  $t$  distributions in the present analysis.

The following requirements are applied for the selection of the  $\tau^+\tau^-$  events where both  $\tau$ -leptons decay into three charged pions and a neutrino:

1. there are exactly six charged pions with zero net charge and there are no other charged tracks;
2. the  $K_S^0$  mesons,  $\Lambda$ -hyperons and  $\pi^0$  are found by  $V^0$  [8] and  $\pi^0$  reconstruction algorithms and the event is discarded if any of these are seen;
3. the number of photons should be smaller than six and their total energy should be less than 0.7 GeV;
4. the thrust value of the event in the CM frame is greater than 0.9;

5. the square of the transverse momentum of the  $6\pi$  system is required to be greater than  $0.25 (\text{GeV}/c)^2$  to suppress the  $e^+e^- \rightarrow e^+e^-6\pi$  two-photon events;
6. the mass  $M(6\pi)$  of the  $6\pi$  system should fulfill the requirement  $4 \text{ GeV}/c^2 < M(6\pi) < 10.25 \text{ GeV}/c^2$  to suppress other background events;
7. there should be three pions (triplet) with net charge equal to  $\pm 1$  in each hemisphere (separated by the plane perpendicular to the thrust axis in the CM);
8. the pseudomass (see the definition in Ref. [9]) of each triplet of pions must be less than  $1.8 \text{ GeV}/c^2$ ;
9. each pion-triplet vertex-fit quality must satisfy  $\chi^2 < 20$ ;
10. the discriminant  $D$  of Eq. (2) should satisfy  $D > -0.05$  (with slightly negative values arising from experimental uncertainties; if this happens, we use  $D = 0$  when solving the equation);
11. the distance of closest approach must satisfy  $dl < 0.03 \text{ cm}$  to reject events with large uncertainties in the reconstructed momenta and vertex positions.

All of these selection criteria are based on a study of the signal and background Monte Carlo (MC) simulated events.

For the signal MC sample, we use  $\tau^+\tau^-$  events produced by the KKMC generator [10] with the mean lifetime  $\langle\tau\rangle = 87.11 \mu\text{m}$  that are then fed to the full detector simulation based on GEANT 3 [11]. These events are passed through the same reconstruction procedures as for the data.

For the background estimation, we use the MC samples of events generated by the EVT-GEN program [12], which correspond to the one-photon annihilation diagram  $e^+e^- \rightarrow q\bar{q}$ , where  $q\bar{q}$  are  $u\bar{u}$ ,  $d\bar{d}$ ,  $s\bar{s}$  ( $uds$  events),  $c\bar{c}$  (charm events), and  $e^+e^- \rightarrow \Upsilon(4S) \rightarrow B^+B^-, B^0\bar{B}^0$  (beauty events). All these events are passed through the full detector simulation and reconstruction procedures. The statistics in these MC samples are equivalent to the integrated luminosity of the data, *i.e.*, the number of events of a given category is equal to the product of the integrated luminosity of the data and the expected cross section from theory. For the estimation of the background from the process  $\gamma\gamma \rightarrow \text{hadrons}$  ( $\gamma\gamma$  events), we use events generated by PYTHIA [13] that are subjected to the afore-mentioned simulation and reconstruction procedures.

In addition to the above MC samples, we also use two  $e^+e^- \rightarrow \tau^+\tau^-$  MC samples, generated by KKMC, where both  $\tau$ -leptons are forced to decay into three charged pions and



a neutrino. The mean lifetimes for these two samples are 84 and 90  $\mu\text{m}$ , which are about  $10\sigma$  below and above the PDG value. These two samples are also passed through the same detector simulation and reconstruction procedures.

### III. ANALYSIS OF THE EXPERIMENTAL RESULTS

In the measured proper time distribution, the exponential behavior is smeared by the experimental resolution. This resolution has been studied with MC simulation. The following samples are used, each one with a slightly different time resolution: with the SVD1 and SVD2 geometries and three different values of the mean  $\tau$ -lepton lifetime. For all MC samples, the resolution function is found to be described well by the expression:

$$\begin{aligned}
 R(\Delta t) &= (1 - A\Delta t)e^{-(\Delta t - t_0)^2/2\sigma^2}, \text{ where} \\
 \Delta t &= t_{\text{reconstructed}} - t_{\text{true}}, \quad \Delta t_0 = \Delta t - t_0, \\
 \sigma &= a + b|\Delta t_0|^{1/2} + c|\Delta t_0| + d|\Delta t_0|^{3/2}
 \end{aligned} \tag{3}$$

The parameters  $t_0$ ,  $a$ ,  $b$ ,  $c$  and  $d$  are allowed to vary freely in the fit, while the asymmetry  $A = 2.5 \text{ cm}^{-1}$  is fixed because of its strong correlation with the lifetime parameter  $\tau$ . An example of the fitting of the resolution distribution for the MC sample with mean  $\tau$ -lepton lifetime equal to 87.11  $\mu\text{m}$  and for the sum of the SVD1- and SVD2-geometry data sets by the function Eq. (3) is shown in Fig. 2. The goodness of fit is  $\chi^2/ndf = 770.8/794$ . In an alternate fit where the parameter  $A$  is allowed to vary freely, its best-fit value is  $(2.5 \pm 0.2) \text{ cm}^{-1}$ . All of the other resolution distributions are described with the same level of quality.

After applying all the selection criteria, the contamination of the background in the data is about two percent. The dominant background arises from  $uds$  events. For these events, all six pions emerge (typically) from one primary vertex and these  $uds$  events are similar to the  $\tau^+\tau^-$  events with zero lifetime. Using the MC, we check that the decay time distributions of  $uds$ -events that pass the selection criteria are well described by the resolution function of Eq. (3). The same behavior is found for  $\gamma\gamma$  events, whose fraction in all the selected events is about  $1.4 \cdot 10^{-4}$ . Other sources of background contribute to the selected data sample at the per mille level.

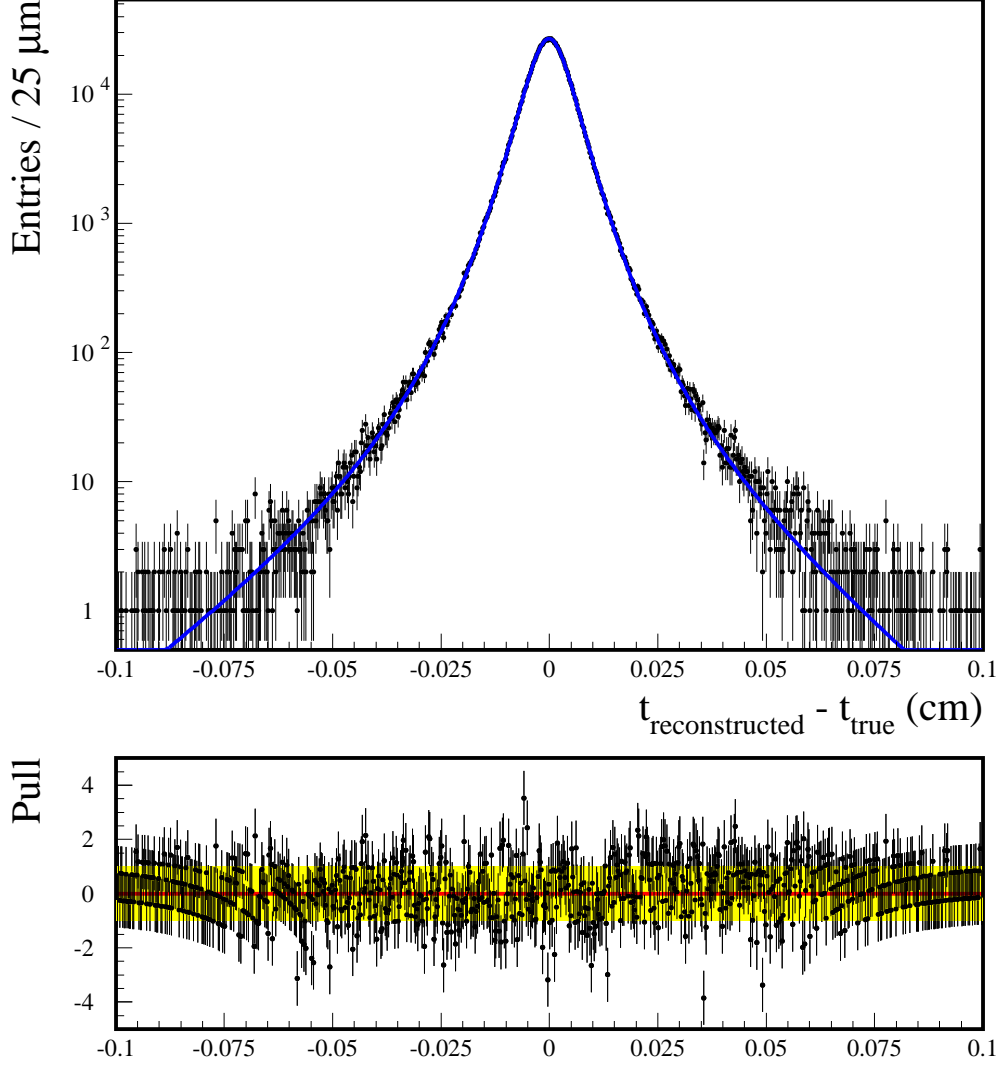


FIG. 2. Distribution of the difference between the reconstructed and true  $t$  values for  $\tau$ -leptons (obtained from an MC sample) for the combined SVD1- and SVD2-geometry data sets. The line is the result of the fit to Eq. (3). The distribution of residuals  $[(\text{data}-\text{fit})/\text{error}]$  for the fit is shown in the bottom panel.

The measured proper time distribution is parameterized by:

$$F(t) = N \int e^{-t'/\tau} R(t-t') dt' + A_{uds} R(t) + B_{cb}(t), \quad (4)$$

where the resolution function  $R(t)$  is given by Eq. (3),  $A_{uds}$  is the normalization of the combined  $uds$  and  $\gamma\gamma$  background and  $B_{cb}(t)$  is the background distribution due to charm and beauty events. The shapes and yields of the backgrounds ( $B_{cb}(t)$ ,  $A_{uds}$ ) are fixed from the MC simulation; the free parameters of the fit are the normalization  $N$ , the  $\tau$ -lepton

lifetime  $\tau$  and the five parameters of the resolution function  $t_0$ ,  $a$ ,  $b$ ,  $c$  and  $d$ .

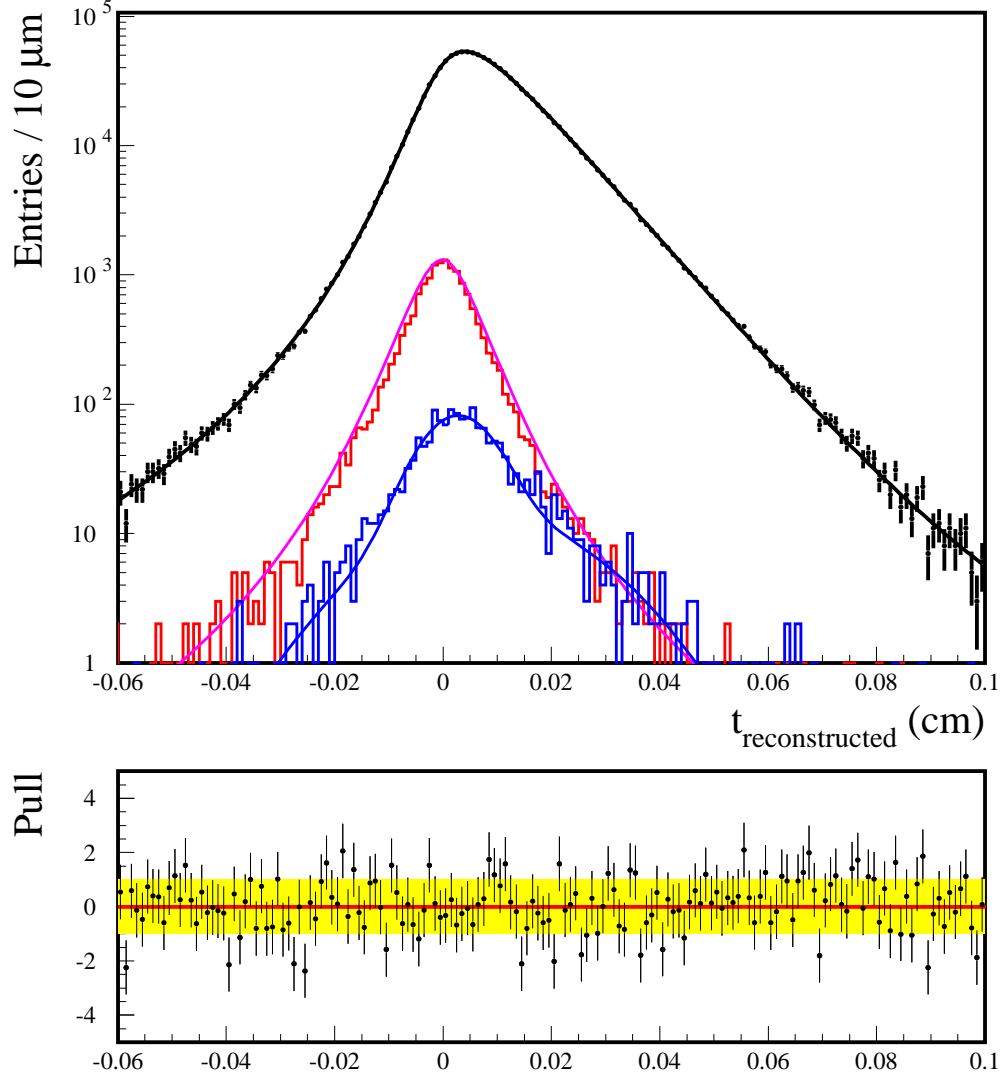


FIG. 3. The measured proper time  $t$  distribution for the data (filled circles with errors). The black line is the result of the fit by Eq. (4). The red histogram is the MC prediction for the sum of the  $uds$  and  $\gamma\gamma$  background contributions. The magenta line is the contribution for  $uds + \gamma\gamma$  obtained in the fit. The blue histogram is the MC prediction for the sum of the charm and beauty background contributions. The blue line is the smoothed distribution of the charm and beauty contributions that is used in the fit. The distribution of residuals  $[(\text{data}-\text{fit})/\text{error}]$  for the fit is shown in the bottom panel.

The result of the fit of the experimental data to Eq. (4) is shown in Fig. 3, together with the contributions from the sum of  $uds$  and  $\gamma\gamma$  events and the sum of charm and beauty events. The curves on these contributions are the result of the fit with Eq. (4),  $A_{uds}R(t)$

function (with fixed value of  $A_{uds}$ ) for  $uds$  plus  $\gamma\gamma$  events and the fixed sum of two Gaussians for charm plus beauty events.

The relation of the parameter  $\tau$  in Eq. (4) to the generated value of the  $\tau$ -lepton mean lifetime is analyzed using three MC  $\tau^+\tau^-$  samples with the mean lifetime values of 84, 87.11 and 90  $\mu\text{m}$ . The dependence of parameter  $\tau$  on the input mean lifetime value  $\langle\tau\rangle$  is found to be linear;  $(\tau - 87) = (0.97 \pm 0.03)(\langle\tau\rangle - 87) + (0.001 \pm 0.07)$  [in units of  $\mu\text{m}$ ] with  $\chi^2$  of 0.2.

Bias arising from the selection criteria is checked by fitting the proper time distribution for the signal MC sample before and after applying cuts, and no bias is found for all the selection criteria listed above. To check that the fitting procedure gives the correct estimation of the input lifetime value for different resolution functions, we perform the fits of the decay time distributions for MC samples with a lifetime of 87.11  $\mu\text{m}$  for the sum of the SVD1 and SVD2 samples, SVD1 and SVD2 samples separately, and for samples with lifetimes equal to 84 and 90  $\mu\text{m}$ . In all cases, the value of the parameter  $\tau$  is equal to the slope of the exponential distribution of the selected events at the generation level within the statistical error of the parameter  $\tau$ .

The value of the parameter  $\tau$  obtained from the fit to the real data is  $86.99 \pm 0.16 \mu\text{m}$ . The conversion of this parameter to the value of the  $\tau$ -lepton mean lifetime using the straight-line parameters of the fit described above gives the same value:  $86.99 \pm 0.16 \mu\text{m}$ . The error here is statistical.

#### IV. ANALYSIS OF SYSTEMATIC UNCERTAINTIES

The following sources of systematic uncertainties are considered and summarized in Table I.

A study of the influence of the SVD misalignment on the systematic shift in the  $\tau$ -lepton lifetime measurement is performed in the following way. We use 4.8 M generated  $\tau^+\tau^-$  events that decay with the  $3\pi\nu_\tau - 3\pi\nu_\tau$  topology and standard Belle SVD alignment. After all selection cuts, about 1.2 M events remain (compared with 1.1 M events in the data). We shift the sensitive elements of SVD along the  $X/Y/Z$  axes by sampling from a Gaussian function with  $\sigma = 10 \mu\text{m}$  and rotation around these axes by sampling from a Gaussian function with  $\sigma = 0.1 \text{ mrad}$ . The values of 10  $\mu\text{m}$  and 0.1 mrad are obtained from the dedicated

TABLE I. Summary of systematic uncertainties

Source	$\Delta\langle\tau\rangle$ ( $\mu m$ )
SVD alignment	0.090
Asymmetry fixing	0.030
Beam energy and ISR/FSR description	0.024
Fit range	0.020
Background contribution	0.010
$\tau$ -lepton mass	0.009
<b>Total</b>	<b>0.101</b>

studies of SVD alignment [7]. We prepare the following decay time MC distributions: with default alignment (4.8 M generated events), one sample with misalignment according to the aforementioned shifts and rotations (4.8 M generated events), several samples with misalignments according to these shifts and rotations with fewer generated events; all these samples have the same events at the generator level. The maximal difference of the parameter  $\tau$  obtained in these fits is  $0.07 \mu m$ . This is due to the possible effect of misalignment and limited MC statistics. We also perform global SVD shifts and rotations with respect to the CDC by  $20 \mu m$  and  $1 \text{ mrad}$ , respectively. The values of  $20 \mu m$  and  $1 \text{ mrad}$  are conservative estimates from the SVD alignment study. The variation of the  $\tau$  parameter is within  $0.06 \mu m$  for these shifts. We take the value  $\sqrt{0.07^2 + 0.06^2} = 0.09 \mu m$  for the systematics due to the SVD misalignment. For an additional check of the alignment of the tracking detectors, we divide our data sample into two non-intersecting samples by the azimuthal ( $\phi$ ) angle of the momentum direction of the positive  $\tau$ -lepton. In the first sample (vertical), the direction of the positive  $\tau$ -lepton should have  $\phi$  between 45 and 135 degrees or between 225 and 315 degrees. The second sample (horizontal) contains all the remaining events. The obtained  $\tau$  parameters are the same within statistical errors, so we do not assign additional systematics due to the azimuthal dependence of the tracking system alignment.

The systematic uncertainty due to fixing the parameter  $A = 2.5 \text{ cm}^{-1}$  is estimated by removing the asymmetry term  $(1 - A\Delta t)$  in the resolution function in Eq. (3). The difference

in the obtained lifetime, which is equal to  $0.03\,\mu\text{m}$ , is taken as a systematic uncertainty.

For the estimation of the accuracy of the initial and final state radiation description by the KKMC generator, we analyze the distributions of  $M(\mu^+\mu^-)c^2 - 2E_{\text{beam}}^*$  for  $e^+e^- \rightarrow \mu^+\mu^-$  events for the data and KKMC events passed through the full Belle simulation and reconstruction procedure. Due to the ISR and FSR, these distributions are asymmetric and their maxima are shifted from zero to the left. If the KKMC description of ISR and FSR energy spectrum is harder or softer than for the data, we would observe the MC peak position shifted from the one in the data. The result of our comparison of the data and MC gives the difference of peak positions between the data and MC of  $(3 \pm 2)\,\text{MeV}$ . We take the relative error  $3\,\text{MeV}/10.58\,\text{GeV} = 2.8 \cdot 10^{-4}$  as a combined uncertainty from the ISR and FSR description, beam energy calibration and the calibration of the tracking system.

The variation of the fit range within about 30% of that shown in Fig. 3 contributes an uncertainty on  $\tau$  of  $\pm 0.02\,\mu\text{m}$ .

The demonstration of the stability of the obtained result to the choice of the selection cuts is shown in Fig. 4. Figure 4a shows the dependence of the fitted parameter  $\tau$  on the value of the cut on  $dl$  for data and MC. Figure 4b shows the measured value of the  $\tau$ -lepton lifetime as a function of the value of the  $dl$ -cut after the linear MC-determined calibration of the parameter  $\tau$ . One can see that this dependence in data is very well reproduced by MC.

During the fit of the real data, the level of the background contribution (parameter  $A_{uds}$ ) is fixed to the nominal value predicted by the MC in a “nominal” fit. The contribution to the systematic error of the  $\langle\tau\rangle$  value due to the uncertainty of the background level is tested by changing the background level in the range of the uncertainty of the  $q\bar{q}$  continuum and other backgrounds, from  $-50\%$  to  $+150\%$ . This range is estimated conservatively from the control sample with looser selection criteria. The maximal variation of the  $\tau$  parameter is  $0.01\,\mu\text{m}$ .

The relative uncertainty due to the accuracy of the  $\tau$ -lepton mass [3] is  $(0.16\,\text{MeV}/c^2)/(1776.82\,\text{MeV}/c^2) = 9.0 \cdot 10^{-5}$ .

To check the stability of the result for the different periods of Belle operation and vertex detector geometries, we repeat the analysis for three subsamples of the data. The obtained results are consistent within statistical errors.

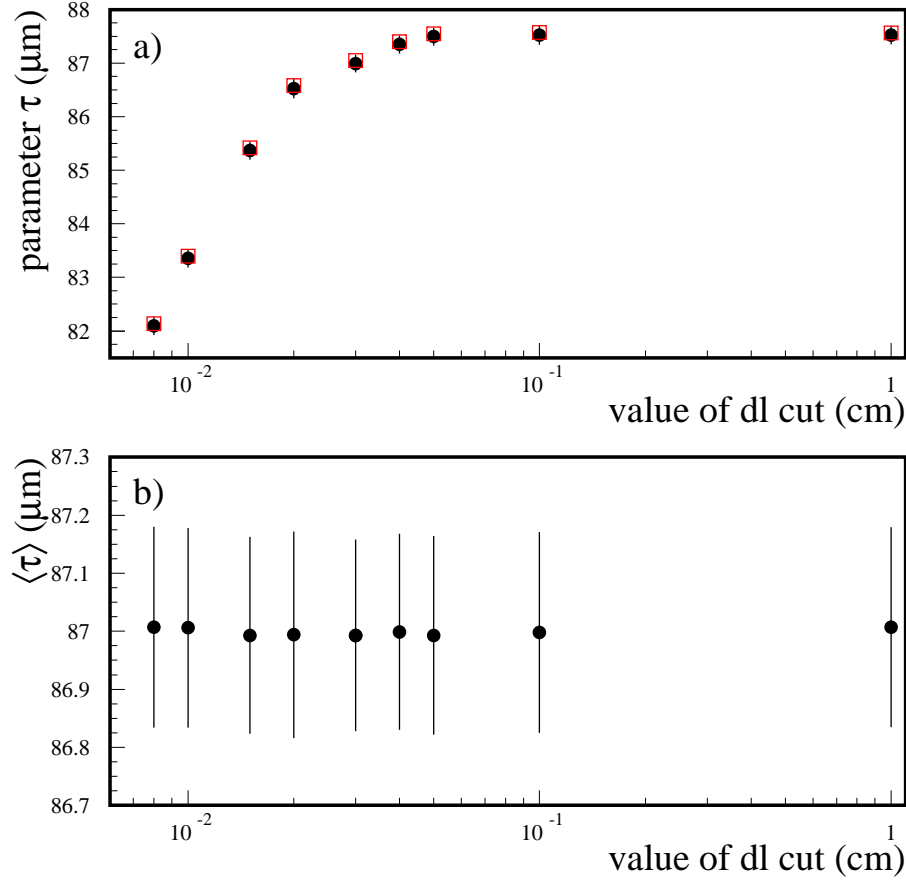


FIG. 4. Stability when varying the value of the  $dl$ -cut. a) The dependence of the fitted parameter  $\tau$  on the value of the  $dl$ -cut for data (filled black circles) and MC (open red squares); the errors are of the same size as the symbols. b) The measured value of the  $\tau$ -lepton lifetime as a function of the value of the  $dl$ -cut; the error bar is the statistical error of the data.

## V. LIFETIME DIFFERENCE BETWEEN POSITIVE AND NEGATIVE $\tau$ -LEPTONS

The present PDG listings provide only the average lifetime of the positive and negative  $\tau$ -leptons. Our measurement determines the lifetimes for positive and negative  $\tau$ -leptons separately. The difference of  $\langle\tau\rangle$  for positive and negative  $\tau$ -leptons obtained in the corresponding fits is  $(0.07 \pm 0.33) \mu\text{m}$ . Most of the sources of systematic uncertainties affect the result for positive and negative  $\tau$ -leptons in the same way, so their contributions to the lifetime difference cancel. The upper limit on the relative lifetime difference is calculated

according to Ref. [14] as

$$|\langle\tau_{\tau+}\rangle - \langle\tau_{\tau-}\rangle|/\langle\tau_{\tau}\rangle < 7.0 \times 10^{-3} \text{ at } 90\% \text{ CL.} \quad (5)$$

The systematic uncertainty of the lifetime difference is at least one order of magnitude smaller than the statistical one, and is neglected.

## VI. CONCLUSIONS

In summary, the  $\tau$ -lepton lifetime has been measured using the technique of the direct decay time measurement in fully kinetically reconstructed  $e^+e^- \rightarrow \tau^+\tau^- \rightarrow 3\pi\nu_{\tau} \ 3\pi\nu_{\tau}$  events. The obtained result for the product of the mean lifetime and speed of light is

$$\langle\tau_{\tau}\rangle = [86.99 \pm 0.16(\text{stat.}) \pm 0.10(\text{syst.})] \mu\text{m}, \quad (6)$$

or in units of seconds

$$(290.17 \pm 0.53(\text{stat.}) \pm 0.33(\text{syst.})) \cdot 10^{-15} \text{ s.}$$

The first measurement of the lifetime difference between  $\tau^+$  and  $\tau^-$  is performed. The obtained upper limit on the relative lifetime difference between positive and negative  $\tau$ -leptons is  $|\langle\tau_{\tau+}\rangle - \langle\tau_{\tau-}\rangle|/\langle\tau_{\tau}\rangle < 7.0 \times 10^{-3}$  at 90% CL.

## VII. ACKNOWLEDGMENTS

We thank the KEKB group for excellent operation of the accelerator; the KEK cryogenics group for efficient solenoid operations; and the KEK computer group, the NII, and PNNL/EMSL for valuable computing and SINET4 network support. We acknowledge support from MEXT, JSPS and Nagoya's TLPRC (Japan); ARC and DIISR (Australia); FWF (Austria); NSFC (China); MSMT (Czechia); CZF, DFG, and VS (Germany); DST (India); INFN (Italy); MEST, NRF, GSDC of KISTI, and WCU (Korea); MNiSW and NCN (Poland); MES and RFAAE (Russia); ARRS (Slovenia); IKERBASQUE and UPV/EHU (Spain); SNSF (Switzerland); NSC and MOE (Taiwan); and DOE and NSF (USA).

---

[1] Y.S. Tsai, Phys. Rev. D **4**, 2821 (1971); H.B. Thacker and J.J. Sakurai, Phys. Lett. B **36**, 103 (1971).



- [2] S. Schael *et al.* [ALEPH and DELPHI and L3 and OPAL and LEP Electroweak Working Group Collaborations], arXiv:1302.3415 [hep-ex].
- [3] J. Beringer *et al.* (Particle Data Group), Phys. Rev. D **86**, 010001 (2012).
- [4] P. Abreu *et al.* (DELPHI Collaboration), Phys. Lett. B **365**, 448 (1996); G. Alexander *et al.* (OPAL Collaboration), Phys. Lett. B **374**, 341 (1996); R. Barate *et al.* (ALEPH Collaboration), Phys. Lett. B **414**, 362 (1997); M. Acciarri *et al.* (L3 Collaboration), Phys. Lett. B **479**, 67 (2000).
- [5] A. Abashian *et al.* (Belle Collab.), Nucl. Instr. and Meth. A **479**, 117 (2002); see also the detector section in J. Brodzicka *et al.*, Prog. Theor. Exp. Phys. (2012) 04D001.
- [6] S. Kurokawa and E. Kikutani, Nucl. Instr. and Meth. A **499**, 1 (2003) and other papers included in this volume;  
T.Abe *et al.*, Prog. Theor. Exp. Phys. (2013) 03A001 and following articles up to 03A011.
- [7] Z. Natkaniec *et al.* (Belle SVD2 Group). Nucl. Instr. and Meth. A **560** 1 (2006).
- [8] K. Sumisawa *et al.* (Belle Collaboration), Phys. Rev. Lett. **95**, 061801 (2005).
- [9] K. Belous *et al.* (Belle Collaboration), Phys. Rev. Lett. **99**, 011801 (2007).
- [10] S.Jadach, B.F.L.Ward and Z.Was, Comp. Phys. Commun. **130**, 260 (2000).
- [11] R. Brun *et al.* GEANT 3.21. Report No. CERN DD/EE/84-1 (1984).
- [12] D.J. Lange, Nucl. Instr. and Meth. A **462**, 152 (2001).
- [13] T. Sjöstrand *et al.*, Comp. Phys. Commun. **135**, 238 (2001).
- [14] G.J. Feldman and R.D. Cousins, Phys. Rev. D **57**, 3873 (1998); J. Conrad *et al.*, Phys. Rev. D **67**, 012002 (2003).